

Exhaust ventilation performance in residential washrooms for bioaerosol particle removal after water closet flushing

K.W. Mui, L.T. Wong*, H.C. Yu, C.T. Cheung, N. Li

Department of Building Services Engineering, The Hong Kong Polytechnic University,

Hong Kong, China

*Corresponding author: L.T. Wong

E-mail: beltw@polyu.edu.hk; Tel: (852) 2766 7783; Fax: (852) 2765 7198

Abstract

Potential bioaerosol infection risk associated with toilet flushing has not been sufficiently addressed in the design of residential washroom exhaust system. This study evaluates the performance of exhaust ventilation for residential washrooms in terms of air change rate, washroom size, washroom geometry, and locations of door louver, exhaust and water closet (WC). Three bioaerosol species namely *Escherichia coli* (ATCC10536), *Serratia marcescens* (ATCC6911) and *Cladosporium cladosporioides* (ATCC16022) are included in the simulations. By shortening the distance between the locations of exhaust and emission source (i.e. WC), the fractional counts of bioaerosol particles exhausted and the time to steady state can be enhanced. An increased air change rate and a louvered door can also improve the exhaust ventilation performance, yet with a longer time to steady state. This study should provide a useful source of reference for washroom exhaust designers to minimize bioaerosol infection risk.

Practical application

This paper shows for residential washroom with an exhaust fan installed, the ventilation performance can be improved by an increased air change rate, and by shortening the distance between the locations of exhaust and emission source.

Keywords

bioaerosol particle, exhaust ventilation, toilet flushing, residential washroom

Highlights

- Exhaust ventilation performance associated with bioaerosol infection risk in residential washrooms.
- Computational fluid dynamics (CFD) simulations of bioaerosol particle dispersion after WC flushing.
- Exhausted bioaerosol particles increased with increasing air change rate.
- Time to steady state shortened by a higher air change rate.
- Exhaust ventilation performance enhanced by a higher local airflow rate near the WC.

Nomenclature

A_b	Projected image area of a bioaerosol particle (μm^2)
ach	Air change rate (h^{-1})
C_D	Drag coefficient
c_o	Theoretical order of convergence
c_{asympt}	Asymptotic range of convergence
d_i	Microbe-laden droplet diameter (μm)
d_b	Equivalent bioaerosol particle diameter (μm)
D_{ex}	Distance from WC to exhaust (m)
F_D	Drag force per unit particle mass per relative velocity ($\text{N s kg}^{-1} \text{m}^{-1}$)
F_x	Additional acceleration force per unit particle mass (N kg^{-1})
f_s	Safety factor
GCI_{coarse}	Grid convergence index for coarse grid
GCI_{fine}	Grid convergence index for fine grid
g	Gravitational acceleration (m s^{-2})
K_D	Drag constant
l_1	Length of a bioaerosol particle (μm)
l_2	Width of a bioaerosol particle (μm)
n_a	Number of bioaerosol particles suspended in the air
n_e	Number of bioaerosol particles removed through exhaust
n_d	Number of bioaerosol particles deposited onto washroom surfaces
n_s	Number of bioaerosol particles emitted from WC
n_w	Number of microorganisms in the WC seal
p	p -value
Re	Reynolds number for bioaerosol particles
r_a	Fractional counts of bioaerosol particles suspended
r_{aspect}	Aspect ratio of bioaerosol particles
r_d	Fractional counts of bioaerosol particles deposited
r_e	Fractional counts of bioaerosol particles exhausted
r_r	Refinement ratio
V_{room}	Room volume (m^3)

v_a	Air velocity (m s^{-1})
v_b	Bioaerosol particle velocity (m s^{-1})
v_{wc}	Air velocity at a height of 0.2 m above the WC seal (m s^{-1})
ε_{rms}	Relative error of computed average mass flow rate
τ	Time (s)
τ_a	Time to steady state (s)
ρ_a	Air density (kg m^{-3})
ρ_b	Density of the bioaerosol particles emitted (kg m^{-3})
μ_a	Molecular viscosity of air ($\text{kg m}^{-1} \text{s}^{-1}$)

1. Introduction

Microorganisms breed rapidly in a warm and humid washroom environment and can live for up to six hours.¹ Human faecal microorganisms such as *Escherichia coli*, *Streptococcus faecalis* and *Serratia marcescens* are commonly found on the seat and under the rim of the water closet (WC).²⁻⁵ They can be spread through splashing during defecation, surface contact and direct inhalation.⁶⁻⁹ In the past, microbial bioaerosol generation was correlated with energy from flushing toilets, water level in the cistern, types of WCs and the number of microorganisms in the WC seal.^{10,11}

Besides source mitigation (e.g. disinfectants, closing the WC lid), mechanical exhaust ventilation is a common infection control measure to remove bioaerosol particles in washrooms.^{12,13} Exhaust system designs for odour dilution at an air change rate are recommended.¹⁴⁻¹⁸ However, current design practice is not quantitatively associated with contaminant removal efficiency, contaminant generation rate, and airflow patterns related to emission source, exhaust location and room geometry.

Using the time-varying fractional counts of bioaerosol particles as indicative parameters, this study evaluates the exhaust ventilation performance for typical residential washrooms.^{17,18} The findings should provide a useful source of reference for washroom exhaust designers to minimize bioaerosol infection risk.

2. Methodology

Figure 1 illustrates a typical ventilation arrangement for a typical residential washroom. Three mechanically ventilated residential washrooms namely Washrooms A,

B and C as listed in Table 1 were studied using computational fluid dynamics (CFD) simulations; the influence of room size, room geometry, door louver and exhaust location on different air change rates were investigated. Washroom A was a typical small washroom (room volume $V_{room}=1.6 \text{ m}^3$) of dimensions $0.90 \text{ m (L)} \times 0.90 \text{ m (W)} \times 2.0 \text{ m (H)}$ as shown in Figure 2, while Washroom B was a typical washroom ($V_{room}=8.9 \text{ m}^3$) measuring $2.35 \text{ m (L)} \times 1.39 \text{ m (W)} \times 2.73 \text{ m (H)}$ and with a bathtub as shown in Figure 3. Washroom C was same as Washroom B but with a door louver of size $0.6 \text{ m (W)} \times 0.3 \text{ m (H)}$ installed. As exhibited in Figure 3, the door louver had 4 air inlet slots, each of size $0.6 \text{ m (W)} \times 0.025 \text{ m (H)}$.

2.1 Numerical simulations

To solve the gas-solid two-phase flow problem, airflow field and bioaerosol particle dispersion in a washroom were determined by the CFD software FLUENT (Version 14) using an Eulerian-Lagrangian framework presented in Figure 4. The Eulerian scheme, which was employed to predict the steady state airflow fields, was followed by the Lagrangian approach that could determine the bioaerosol movements. The renormalization group (RNG) k - ϵ turbulence model and the pressure implicit with splitting of operator (PISO) algorithm were adopted from a previous study.¹⁹

Three reference grid sizes namely fine, moderate and coarse (with mesh skewnesses <0.25 , double- and quadruple-fine respectively) were used to examine the mesh quality based on linear grid stretching. Grid convergence indexes (GCIs) given by Equation (1), where f_s is the safety factor, r_r is the refinement ratio, ϵ_{rms} is the relative error of computed

average mass flow rate and c_o is the theoretical order of convergence, were applied to check the asymptotic range of convergence c_{asympt} at unity.²⁰ The GCI analysis results for subsequent calculations are summarized in Table 2.

$$c_{asympt} = \frac{GCI_{coarse}}{(GCI_{fine})r_r^{c_o}}; GCI_{fine} = \frac{f_s |\mathcal{E}_{rms}|}{(r_r^{c_o} - 1)}; GCI_{coarse} = \frac{f_s |\mathcal{E}_{rms}| r_r^{c_o}}{(r_r^{c_o} - 1)} \quad (1)$$

Airflow simulation results were validated with on-site measurements of air velocity v_a (by TSI 8475 Air Velocity Transducer) at the exhaust terminal position A1 in all washrooms under an air change rate ach in between 7 h⁻¹ and 12 h⁻¹. No significant differences were reported between measured and simulated average velocities for Washroom A ($n=92, p>0.8, t-test$) and Washroom C ($n=36, p>0.7, t-test$).

2.2 Bioaerosol particles generated, dispersed, deposited and exhausted

Three species including *Escherichia coli* (ATCC 10536), *Serratia marcescens* (ATCC 6911) and *Cladosporium cladosporioides* (ATCC 16022) were used in the simulations. Table 3 summarizes their parameter details. Their equivalent bioaerosol particle diameters d_b (μm) are given by Equation (2), where r_{aspect} is the aspect ratio of bioaerosol particles, l_1 (μm), l_2 (μm) and A_b (μm^2) are respectively the length, width and projected image area of a bioaerosol particle determined from scanning electron microscope (SEM) images.²¹

$$d_b = 2\sqrt{\frac{A_b}{\pi}}; r_{aspect} = \frac{\max(l_1, l_2)}{\min(l_1, l_2)} \quad (2)$$

According to Gerba, Wallis, and Melnick,¹¹ for an assumed average faecal weight of 100 g at a microorganism concentration level of 10⁸ g⁻¹ in the WC seal, the number of

bioaerosol particles emitted into the air n_s after a toilet flush was estimated to be 17,160.(2) By assuming that all bioaerosol particles were emitted uniformly from the water surface of the WC seal,^{1,11} each particle was tracked separately for its position and velocity using a discrete phase model (DPM). For predicting the bioaerosol particle movements with one-way coupling in the simulated airflow fields, the particles were assumed to have no effect on the continuum airflow.

The dispersion of bioaerosol particles in the simulated airflow fields can be described by the force balance on the particles and the change of particle velocity v_b (m s^{-1}) under the Lagrangian scheme. It is expressed by Equation (3), where v_a is the air velocity (m s^{-1}), g is the gravitational acceleration (m s^{-2}), F_D is the drag force per unit particle mass per relative velocity ($\text{N s kg}^{-1} \text{ m}^{-1}$), F_x is the additional acceleration force per unit particle mass (N kg^{-1}), ρ_b (i.e. $1,100 \text{ kg m}^{-3}$) is the density of the bioaerosol particles emitted (kg m^{-3}), ρ_a is the air density (kg m^{-3}), μ_a is the molecular viscosity of air ($\text{kg m}^{-1} \text{ s}^{-1}$), Re is the Reynolds number and C_D is the drag coefficient.²²

$$\frac{dv_b}{d\tau} = F_D(v_a - v_b) + \frac{g(\rho_b - \rho_a)}{\rho_b} + F_x; F_D = \frac{18\mu_a}{d_b^2\rho_b} \times \frac{C_D Re}{24}; Re = \frac{\rho_a d_b |v_b - v_a|}{\mu_a} \quad (3)$$

The transient process from droplets (emitted from the WC) to droplet nuclei due to evaporation takes place within a short period of time ($<0.1 \text{ s}$).^{23,24} On the assumption that the droplet nuclei contained infectious pathogens, the equivalent bioaerosol diameters d_b presented in Table 3 were adopted in the simulations. The drag coefficient C_D of a bioaerosol particle (in droplet nuclei) is given by the following expression, where K_D is the bioaerosol particle drag constant,²¹

$$C_D = \frac{K_D}{Re}; Re < 1; K_D = \frac{d_b^2}{2}; 0.69 \mu m \leq d_b \leq 6.9 \mu m \quad (4)$$

A previous study confirmed that the isotropic discrete random walk (DRW) model is effective and accurate in modelling the dispersion and distribution of bioaerosol particles due to turbulent fluctuations in the flow.¹⁹ Hence, a very low volume fraction ($<3,000 \text{ cm}^{-3}$) was kept in the washrooms of this study to reduce the collision of bioaerosol particles in turbulent flows.^{25,26}

For bioaerosol particle deposition, a perfect sink boundary was applied to the washroom surfaces in order that the impinging particles would be perfectly trapped with no reflection and desorption. The number of the bioaerosol particles exhausted or deposited onto the washroom surfaces can be counted.

The proposed computational approach was tested and the simulated bioaerosol particle deposition patterns were compared with the experimental data from the open literature for model verification.^{8,11} Mesh sizes for the test cases and the simulation results are exhibited in Tables 2 and 4 respectively. No significant difference in microorganism counts was found between the simulation and measurement results ($p > 0.26$, *chi-square test*). The computational simulation framework proposed was thus tested suitable for this study.

2.3 Exhaust ventilation performance

Bioaerosol particles (in counts) generated from the WC n_s will suspend in the air n_a , deposit on washroom surfaces n_d or be removed through the exhaust vent n_e . The time-varying fractional counts of bioaerosol particles $r(\tau)$ as illustrated in Figure 5 are defined

below, where r_e , r_a and r_d are the fractional counts of bioaerosol particles exhausted, suspended and deposited respectively,

$$\frac{n_e}{n_s} + \frac{n_a}{n_s} + \frac{n_d}{n_s} = r_e + r_a + r_d = 1 \quad (5)$$

The time to steady state τ_a (s) can be determined at $r_a(\tau_a)=0$.

3. Results and discussion

Figure 6 shows that the fractional counts of bioaerosol particles exhausted r_e in Washroom A increased with the air change rate ach and became saturated when ach was about $\geq 7 \text{ h}^{-1}$. According to Figure 7, the time to steady state τ_a was at its peak (up to 600 s) at $ach \leq 6 \text{ h}^{-1}$ in all simulation cases. A shorter τ_a , which was associated with a higher ach and remained steady at $ach \geq 10 \text{ h}^{-1}$, could reduce the risk of infection through inhalation. As shown in Figure 8, similar observations were recorded in Washrooms B and C.

Based on the average fractional counts of bioaerosol particles graphed in Figure 9, room volume had a significant influence on the steady state $r_e(\tau_a)$ and some influence on τ_a . As presented in Figure 10(a), $r_e(\tau_a)$ at $ach=9 \text{ h}^{-1}$ was halved from 0.6 (Washroom A) to 0.3 (Washroom B) when the room volume increased from 1.9 m^3 (Washroom A) to 8.9 m^3 (Washroom B).

Figure 10(b) demonstrates that 150% times τ_a could be reached in Washroom B for an ach range of 4 to 7 h^{-1} . However, as shown in the figure, no significant τ_a difference was found at a higher ach ($\geq 9 \text{ h}^{-1}$).

A higher value of r_e was also associated with the installation of a door louver. As illustrated in Figures. 9 and 10(a), the results from Washroom C were a double of those from Washroom B and were very similar to those from Washroom A. At the same time, because of the higher local air speed that could promote local air mixing and lead to a longer suspension time, a much longer time was required to reach the steady state (up to 160% of τ_a) in Washroom C (Figure 10(b)).

The effects of the door louver on r_e and τ_a can be better illustrated using the local air speeds near the water surface of the WC seal. Figure 11 graphs the air velocities at a height of 0.2 m above the WC seal v_{wc} for all washrooms. Figure 12 demonstrates that air speeds in Washrooms A and C were compatible due to the similar amounts of bioaerosol particles transported from the WC to the exhaust. It can be seen that a door louver can alter airflow paths and a properly positioned air inlet can enhance local airflow close to the WC.

Figure 13 shows the decay characteristics for $r_e(\tau_a)$ against the distance from the WC to the exhaust vent D_{ex} in all washrooms. Expectedly, the fractional counts decreased with increasing distance. They became saturated for $ach > 7 \text{ h}^{-1}$ while dropping for $ach \leq 7 \text{ h}^{-1}$. Apart from an increased air change rate, an exhaust vent close to the emission source (i.e. the WC) could improve the efficiency of bioaerosol particle removal.

4. Conclusion

Potential bioaerosol infection risk associated with toilet flushing has not been sufficiently addressed in the design of residential washroom exhaust system. This study evaluated the performance of exhaust ventilation for residential washrooms in terms of air

change rate, washroom size, washroom geometry, and locations of door louver, exhaust and WC. Three bioaerosol species namely *Escherichia coli* (ATCC10536), *Serratia marcescens* (ATCC6911) and *Cladosporium cladosporioides* (ATCC16022) were included in the simulations. By shortening the distance between the locations of exhaust and emission source (i.e. WC), the fractional counts of bioaerosol particles exhausted and the time to steady state can be enhanced. An increased air change rate and a louvered door can also improve the exhaust ventilation performance, yet with a longer time to steady state. This study should provide a useful source of reference for washroom exhaust designers to minimize bioaerosol infection risk.

Acknowledgement

This research project was partially funded by the Public Policy Research Funding Scheme from the Central Policy Unit of the HKSAR Government (Project No.: 2014.A6.038.14E), the Research Grants Council of the HKSAR, China (PolyU 5272/13E) and The Hong Kong Polytechnic University (Project Nos.: GYBA7, GYM64).

List of figures

- 1 Typical ventilation arrangement for a typical residential washroom
- 2 Ventilation arrangement for Washroom A
- 3 Ventilation arrangement for Washrooms B and C
- 4 Computational simulation framework
- 5 Time-varying fractional counts of bioaerosol particles
- 6 Exhausted r_e against air change rate ach in Washroom A
- 7 Time to steady state τ_a against air change rate ach in Washroom A
- 8 Exhausted r_e and time to steady state τ_a against air change rate ach in Washrooms B and C
- 9 Fractional counts of bioaerosol particles r against time τ
- 10 Exhausted r_e and time to steady state τ_a against air change rate ach
- 11 Air velocity at a height of 0.2 m above the WC seal v_{wc}
- 12 Simulated air velocity distribution
- 13 Exhausted r_e against distance from WC to exhaust D_{ex}

List of tables

- 1 Three mechanically ventilated residential washrooms
- 2 Analysis results of grid convergence index (GCI)
- 3 Information of the bioaerosol particles emitted by toilet flushing
- 4 Deposition of microorganisms in two experiments from the open literature

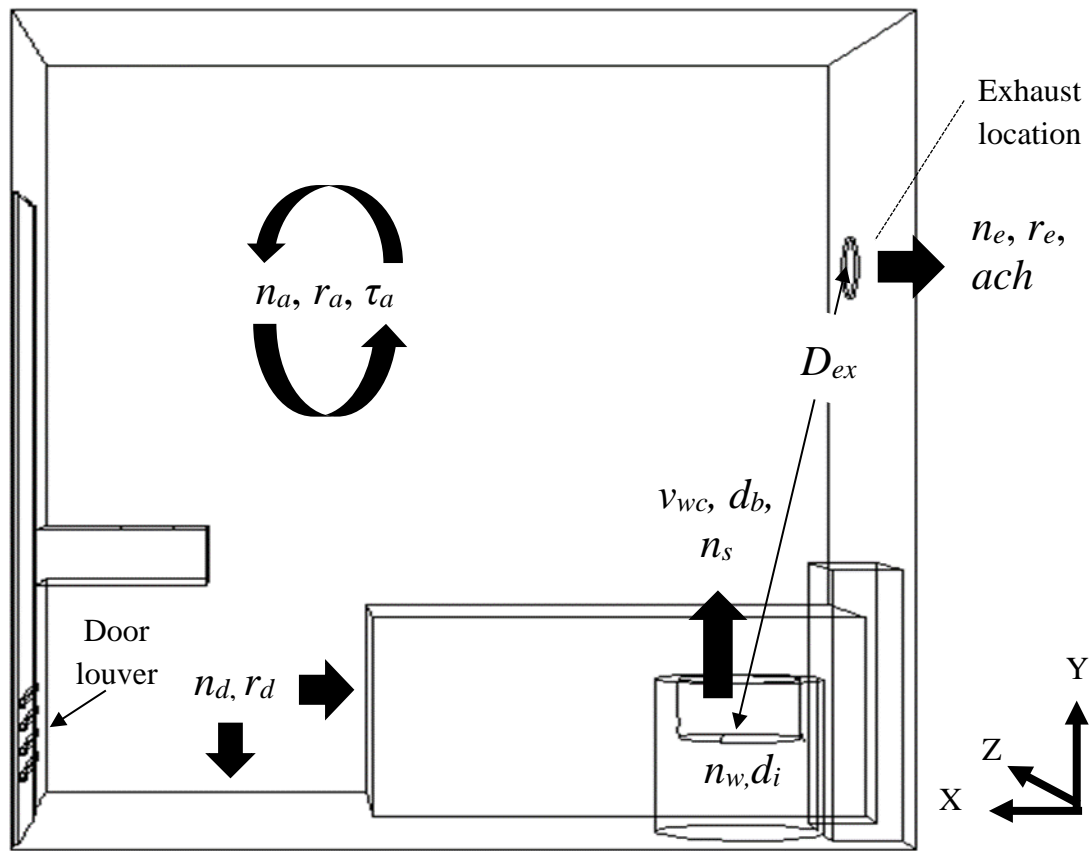


Figure 1. Typical ventilation arrangement for a typical residential washroom

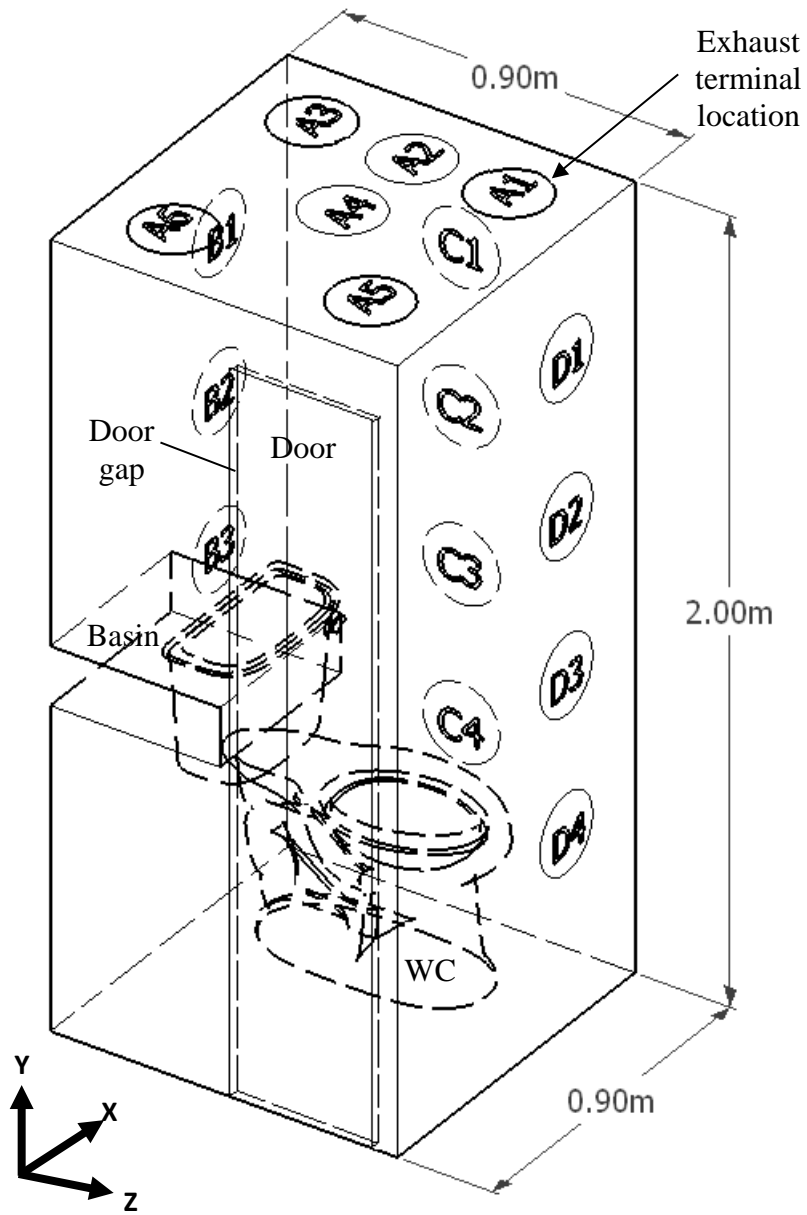


Figure 2. Ventilation arrangement for Washroom A

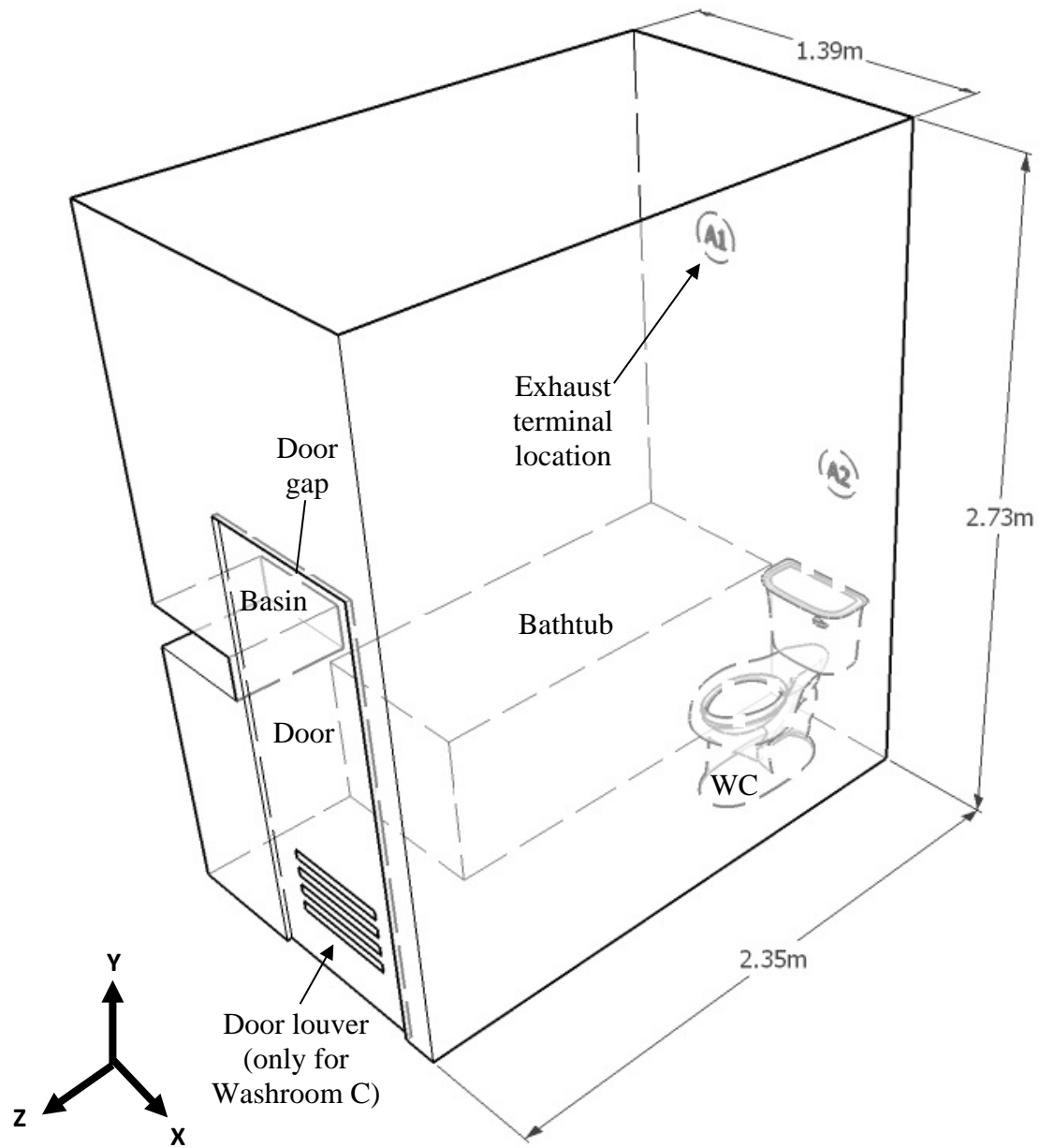


Figure 3. Ventilation arrangement for Washrooms B and C

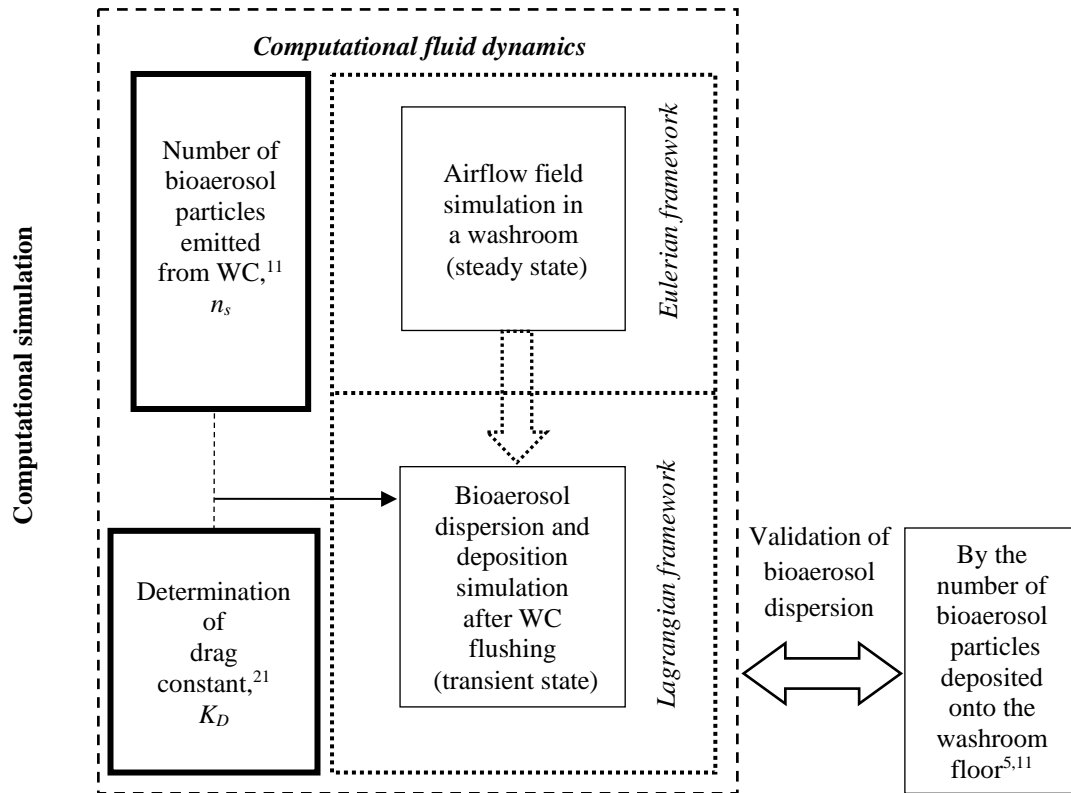


Figure 4. Computational simulation framework

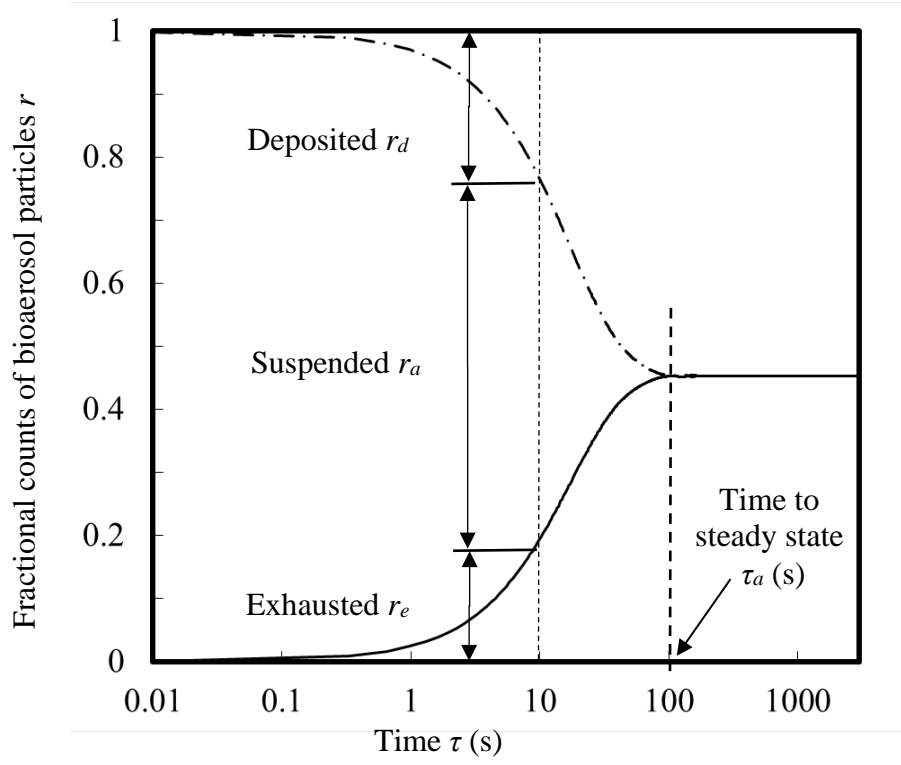


Figure 5. Time-varying fractional counts of bioaerosol particles

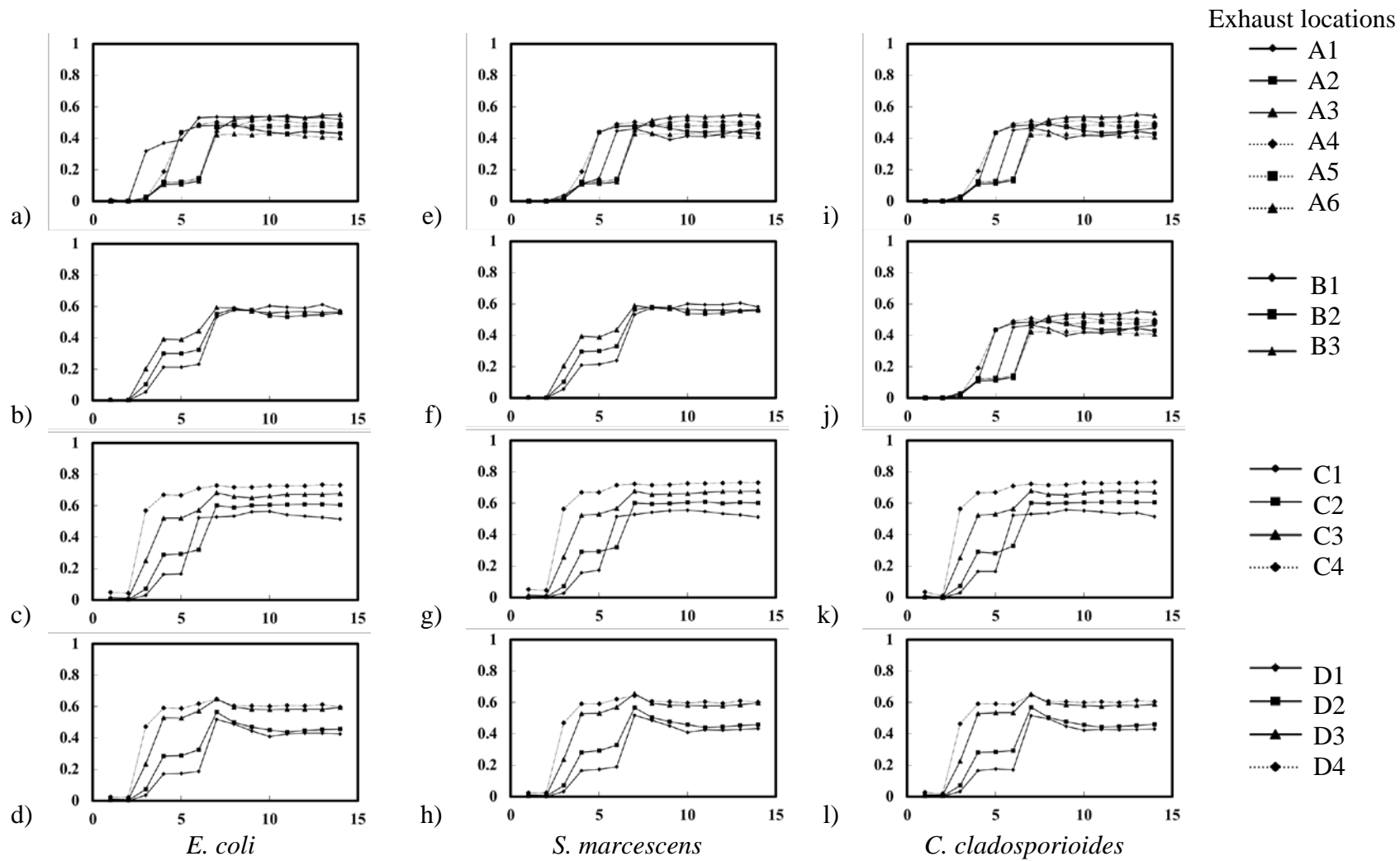


Figure 6. Exhausted r_e against air change rate ach in Washroom A

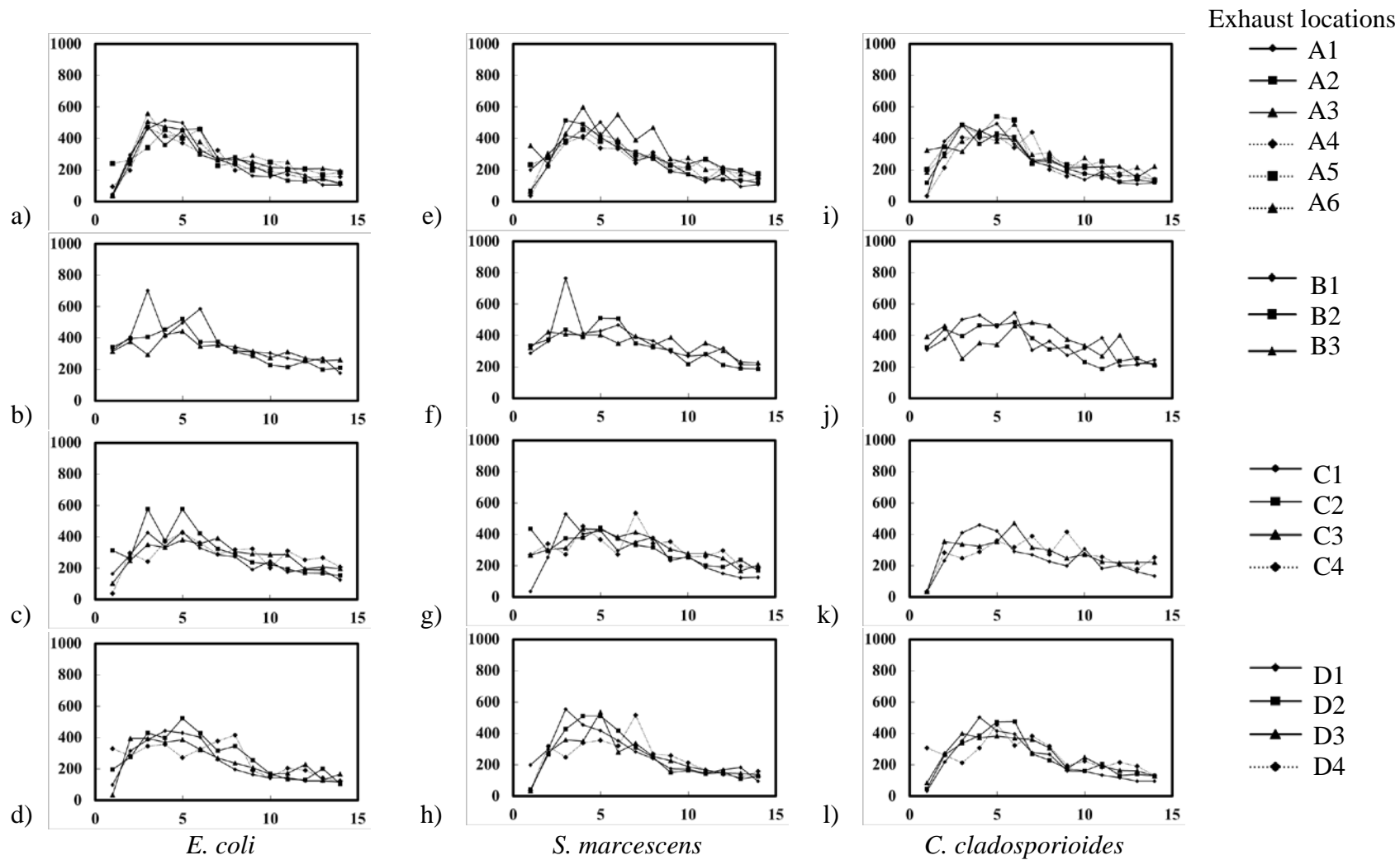
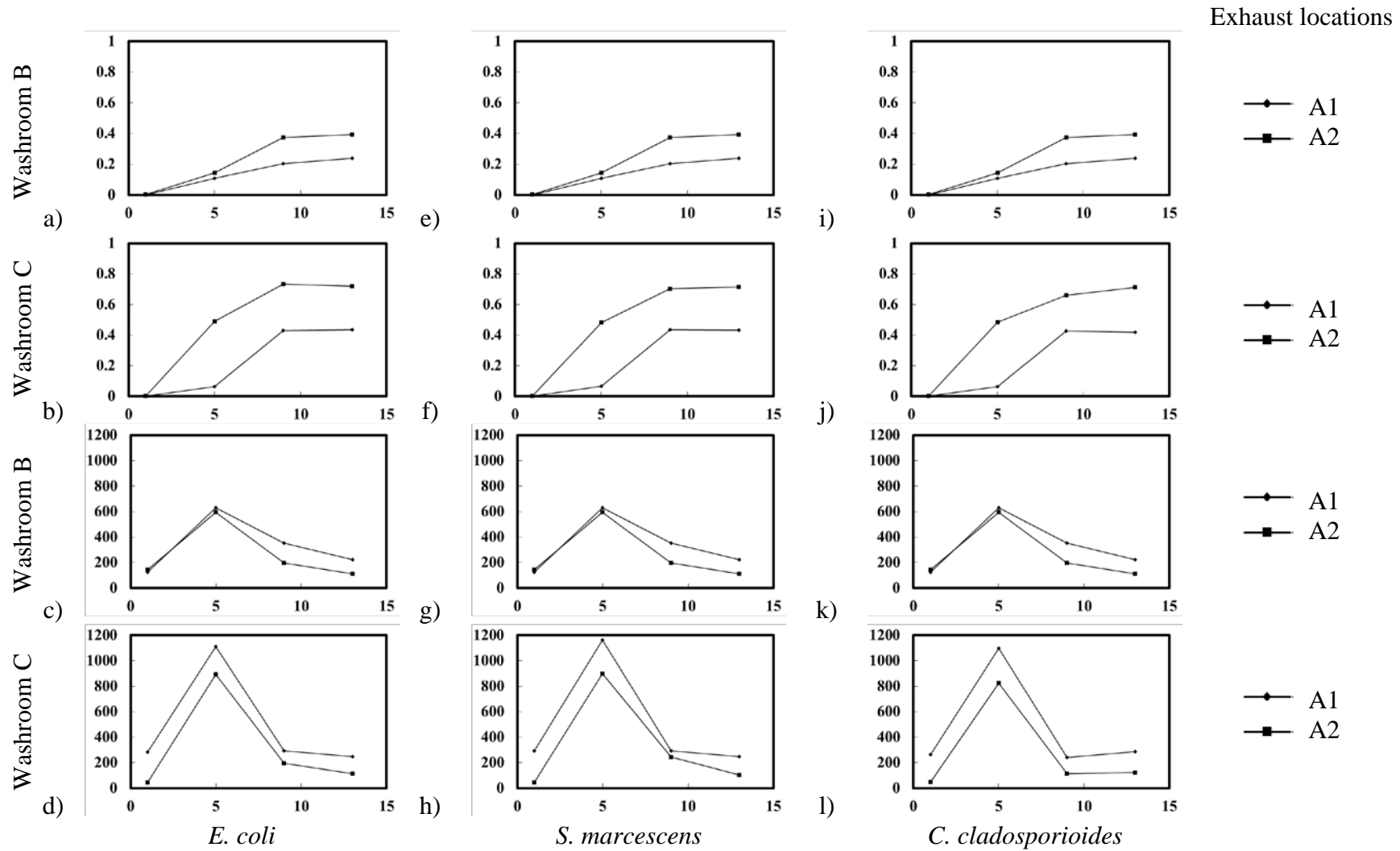


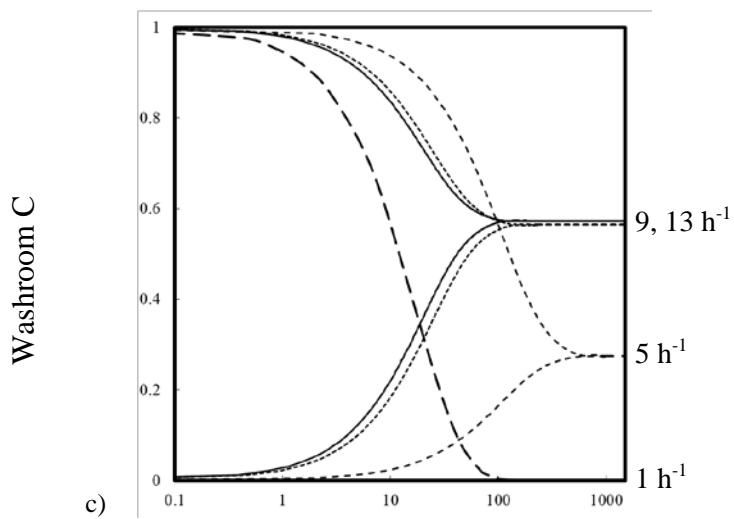
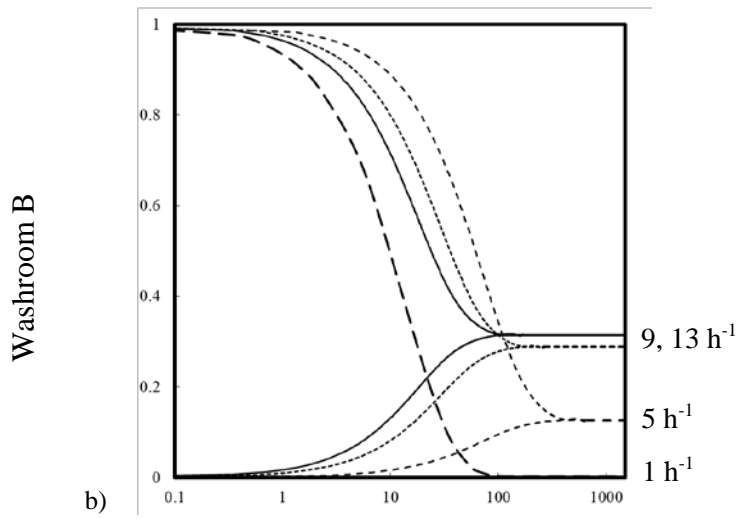
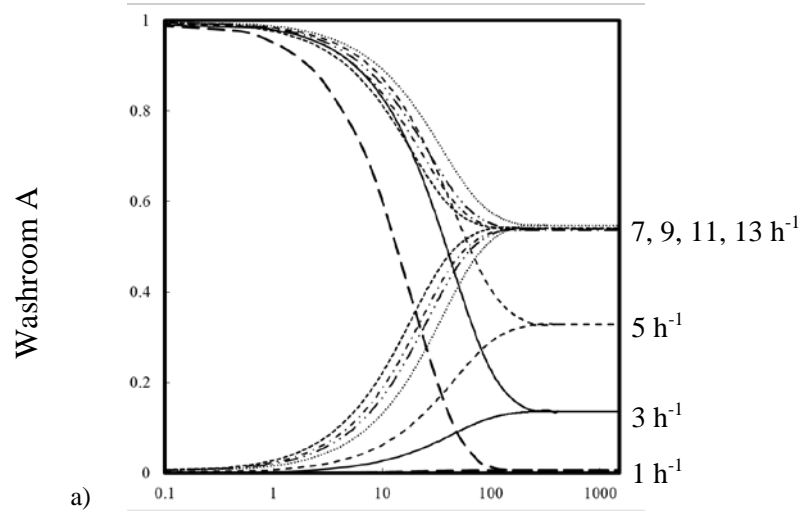
Figure 7. Time to steady state τ_a against air change rate ach in Washroom A



x-axis: Air change rate ach (h^{-1})

y-axis: Exhausted r_e , time to steady state τ_a (s)

Figure 8. Exhausted r_e and time to steady state τ_a against air change rate ach in Washrooms B and C



x-axis: Time τ (s)

y-axis: Fractional counts of bioaerosol particles r

Figure 9. Fractional counts of bioaerosol particles r against time τ

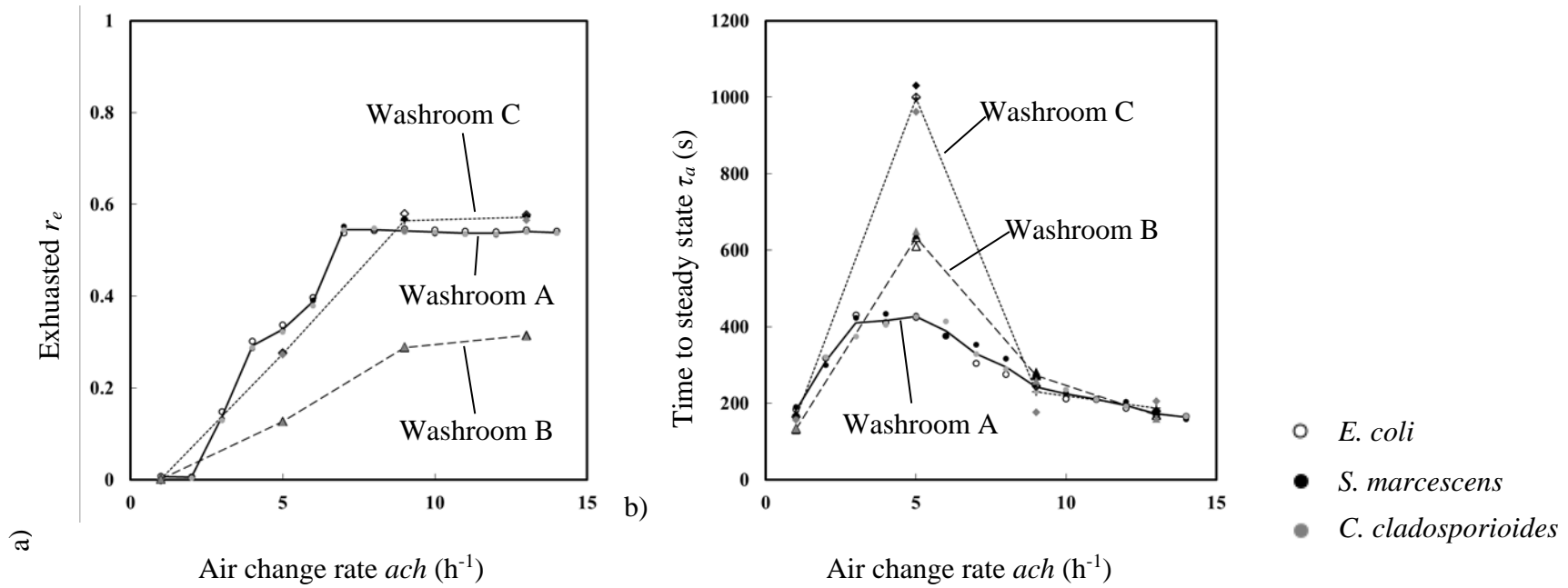


Figure 10. Exhausted r_e and time to steady state τ_a against air change rate ach

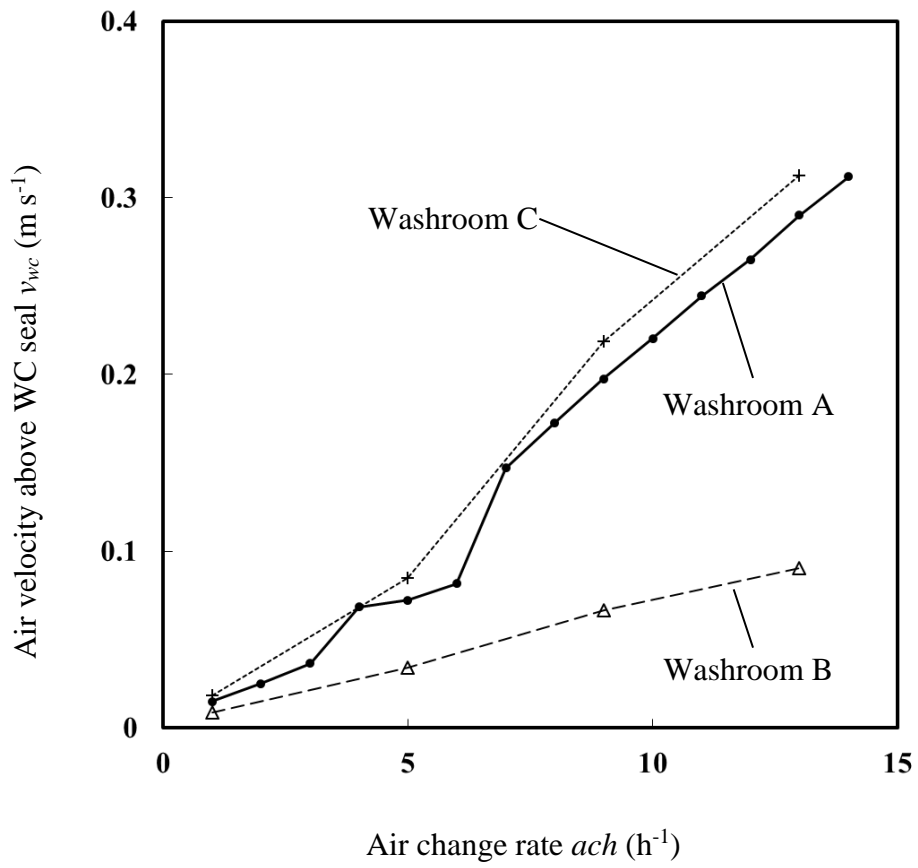


Figure 11. Air velocity at a height of 0.2 m above the WC seal v_{wc}

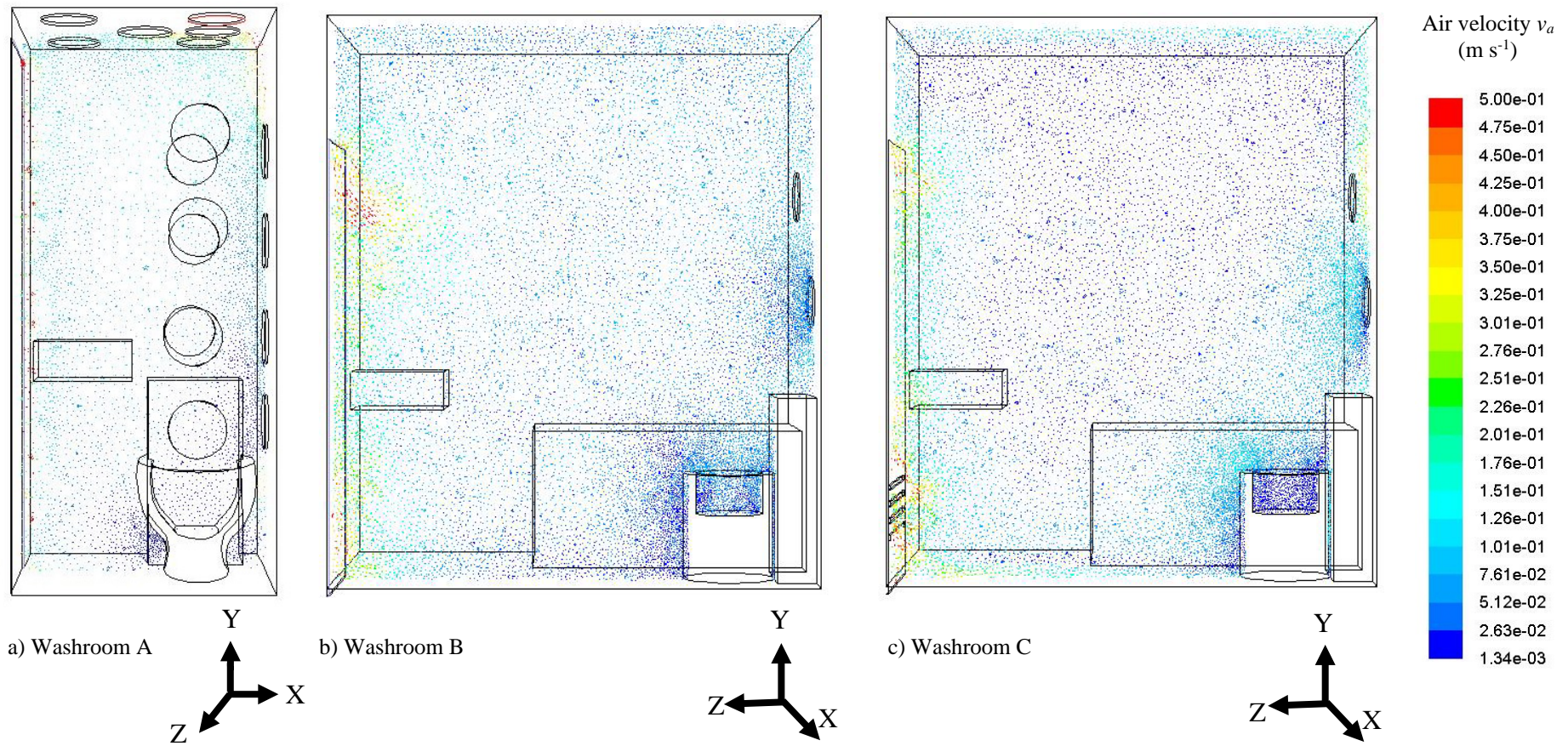
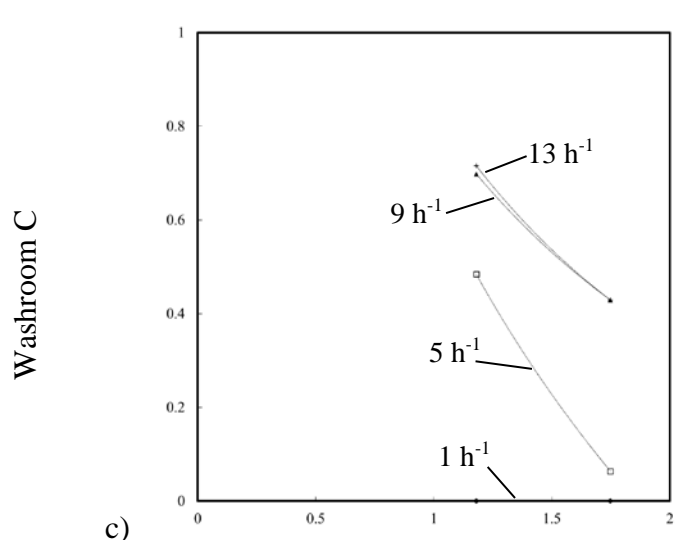
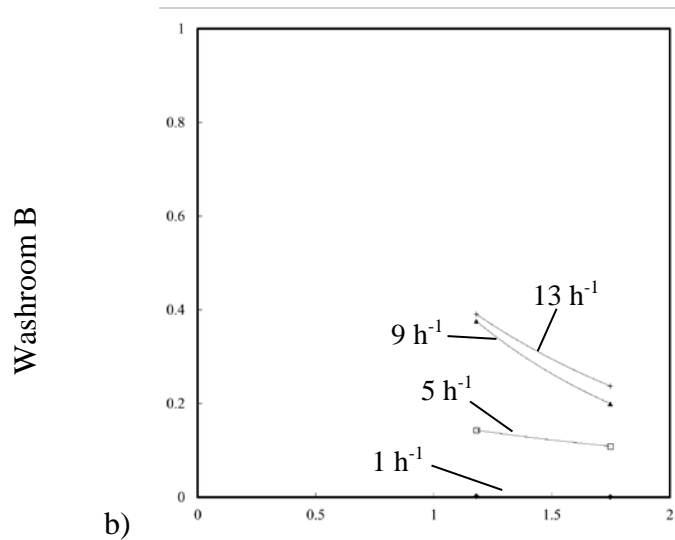
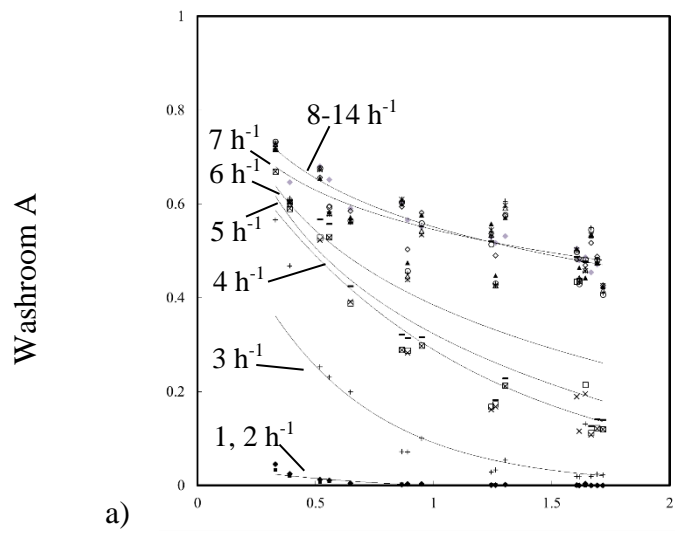


Figure 12. Simulated air velocity distribution



x-axis: Distance D_{ex} (m)
 y-axis: Exhausted r_e

Figure 13. Exhausted r_e against distance from WC to exhaust D_{ex}

Table 1.
Three mechanically ventilated residential washrooms

Washroom	Room volume V_{room} (m³)	Door louver area (m²)	Door size (H × W)	Exhaust distance D_{ex} (m)	Air change rate ach (h⁻¹)
A	1.6	0	1.9 m (H) × 0.54 m (W)	0.33-1.72	1-14
B	8.9	0	2.2 m (H) × 0.7 m (W)	1.18-1.75	1-13
C	8.9	0.18	2.2 m (H) × 0.7 m (W)	1.18-1.75	1-13

Table 2.

Analysis results of grid convergence index (GCI)

Simulation	Selected mesh size	Coarse mesh size	Medium mesh size	Fine mesh size	GCI for coarse grid GCI_{coarse}	GCI for fine grid GCI_{fine}	Asymptotic range of convergence C_{asympt}
Gerba, Wallis, and Melnick ¹¹	60k	16k	60k	204k	53%	56%	0.96
Barker and Jones ⁵	94k	60k	94k	184k	0.008%	4%	0.97
Washroom A	78k	38k	78k	206k	8.6%	23.3%	1.1
Washroom B	276k	271k	276k	317k	20%	1%	1.2
Washroom C	276k	271k	276k	317k	20%	1%	1.2

Table 3.Information of the bioaerosol particles emitted by toilet flushing^{5,11,21}

Species	ATCC	Microbe-laden droplet diameter d_i (μm)	Equivalent bioaerosol particle diameter d_b (μm)	Aspect ratio r_{aspect}	Drag constant K_D	Evaporation time at 0% RH (s)	Evaporation time at 50% RH (s)	Evaporation time at 90% RH (s)
<i>Escherichia coli</i>	10536	1.027	1.0±0.07	1.7	0.5	3.06×10^{-5}	1.3×10^{-4}	1.81×10^{-2}
<i>Serratia marcescens</i>	6911	2.69	2.6±0.07	6.9	3.38	1.99×10^{-4}	1.32×10^{-3}	3.48×10^{-2}
<i>Cladosporium cladosporioides</i>	16022	-	3.4±0.09	2.1	5.78	-	-	-

Table 4.Deposition of microorganisms in two experiments from the open literature^{5,11}

Experiment	Seeding Bacteria	Location	Measurement	Simulation
Gerba, Wallis, and Melnick ¹¹	<i>E. coli</i>	Number of microorganisms on washroom floor	983	970
		Shelf*	14±8	12.7±2.5
		Cistern*	11.5±4.5	10±4.6
Barker and Jones ⁵	<i>S. marcescens</i>	Seat – left*	20±8	22±4.4
		Seat – right*	24.5±4	18.7±4.2
		In front of WC*	11±2.5	5.7±0.6

*Colony-forming unit (CFU) per plate

Reference

- 1 Newsom SWB. Microbiology of hospital toilets. *The Lancet* 1972; 300(7779): 700-3.
- 2 Flores GE, Bates ST, Knights D, Lauber CL, Stombaugh J, Knight R, et al. Microbial biogeography of public restroom surfaces. *PLoS ONE* 2011; 6(11): e28132.
- 3 Irvine RA, Robertson WB. Infection and the water-closet. *Brit Med J* 1964; 1(5397): 1523-4.
- 4 Barker J, Bloomfield SF. Survival of Salmonella in bathrooms and toilets in domestic homes following salmonellosis. *J Appl Microbiol* 2000; 89(1): 137-44.
- 5 Hathway EA, Noakes CJ, Sleigh PA, Fletcher LA. CFD simulation of airborne pathogen transport due to human activities. *Build Environ* 2011; 46(12): 2500-11.
- 6 Burgess JA. Trichomonas Vaginalis infection from splashing in water closets. *The Brit J Vener Dis* 1963; 39: 248-50.
- 7 Darlow HM, Bale WR. Infective hazards of water-closets. *The Lancet* 1959; 273(7084): 1196-200.
- 8 Barker J, Jones MV. The potential spread of infection caused by aerosol contamination of surfaces after flushing a domestic toilet. *J Appl Microbiol* 2005; 99(2): 339-47.
- 9 Sze-To GN, Yang Y, Kwan JKC, Yu SCT, Chao CYH. Effects of surface material, ventilation, and human behavior on indirect contact transmission risk of respiratory infection. *Risk Anal* 2013; 34(5): 818-30.
- 10 Bound WH, Atkinson RI. Bacterial aerosol from water closets. *The Lancet* 1966; 287(7451): 1369-70.
- 11 Gerba CP, Wallis C, Melnick JL. Microbiological hazards of household toilets: droplet production and the fate of residual organisms. *Appl Microbiol* 1975; 30(2): 229-37.
- 12 Mendes MF, Lynch DJ. Bacteriological survey of washrooms and toilets. *J Hyg* 1976; 76(2): 183-90.
- 13 Johnson DL, Mead KR, Lynch RA, Hirst DVL. Lifting the lid on toilet plume aerosol: A literature review with suggestions for future research. *Am J Infect Control* 2013;41(3):254-8.
- 14 Chung K-C, Chiang C-M, Wang W-A. Predicting contaminant particle distributions to evaluate the environment of lavatories with floor exhaust ventilation. *Build Environ* 1997; 32(2): 149-59.
- 15 Tung Y-C, Hu S-C, Tsai T-Y. Influence of bathroom ventilation rates and toilet location on odor removal. *Build Environ* 2009; 44(9): 1810-7.
- 16 Tung Y-C, Shih Y-C, Hu S-C, Chang Y-L. Experimental performance investigation of ventilation schemes in a private bathroom. *Build Environ* 2010; 45(1): 243-51.
- 17 ASHRAE. *Standard 62.1 - 2013. Ventilation for acceptable indoor air quality*. Atlanta, GA: American Society of Heating, Refrigerating and Air-Conditioning Engineers, Inc.; 2013.
- 18 CIBSE. *Heating, ventilating, air conditioning and refrigeration: CIBSE Guide B*. London, England: Chartered Institution of Building Services Engineers; 2005.
- 19 Lai ACK, Wong LT, Mui KW, Chan WY, Yu HC. An experimental study of bioaerosol (1-10um) deposition in a ventilated chamber. *Build Environ* 2012; 56: 118-26.
- 20 Roache PJ. Verification of Codes and Calculations. *AIAA J*. 1998; 36(5): 696-702.
- 21 Wong LT, Yu HC, Mui KW, Chan WY. Drag constants of common indoor bioaerosols. *Indoor Built Environ* 2015; 24(3): 401-13.

- 22 ANSYS. *ANSYS Fluent Theory Guide 14.0*. Canonsburg, PA, USA: ANSYS Inc.; 2011.
- 23 Xie X, Y. L, Chwang ATY, Ho PL, Seto WH. How far droplets can move in indoor environments – revisiting the Wells evaporation–falling curve. *Indoor air* 2007; 17(3): 211-25.
- 24 Yang Y, Sze-To GN, Chao CYH. Estimation of the Aerodynamic Sizes of Single Bacterium-Laden Expiratory Aerosols Using Stochastic Modeling with Experimental Validation. *Aerosol Sci Tech* 2012; 46(1): 1-12.
- 25 Hussein T, Hruska A, Dohanyosova P, Dzumbova L, Hemerka J, Kulmala M, et al. Deposition rates on smooth surfaces and coagulation of aerosol particles inside a test chamber. *Atmos Environ* 2009; 43: 905-14.
- 26 Rim D, Green M, Wallace L, Persily A, Choi JI. Evolution of Ultrafine Particle Size Distributions Following Indoor Episodic Releases: Relative Importance of Coagulation, Deposition and Ventilation. *Aerosol Sci Tech* 2012; 46: 494-503.